Acta Polytechnica CTU Proceedings **2**(1): 205–211, 2015 doi: 10.14311/APP.2015.02.0205

Theory of Nova Outbursts and Type Ia Supernovae

M. Kato[1], I. Hachisu[2]

[1] *Department of Astronomy, Keio University, Hiyoshi, Yokohama 223-8521, Japan*

[2] *Department of Earth Science and Astronomy, College of Arts and Sciences, The University of Tokyo, Komaba, Meguro-ku, Tokyo 153-8902, Japan*

Corresponding author: mariko@educ.cc.keio.ac.jp

Abstract

We briefly review the current theoretical understanding of the light curves of novae. These curves exhibit a homologous nature, dubbed the universal decline law, and when time-normalized, they almost follow a single curve independently of the white dwarf (WD) mass or chemical composition of the envelope. The optical and near-infrared light curves of novae are reproduced mainly by free-free emission from their optically thick winds. We can estimate the WD mass from multiwavelength observations because the optical, UV, and soft X-ray light curves evolve differently and we can easily resolve the degeneracy of the optical light curves. Recurrent novae and classical novae are a testbed of type Ia supernova scenarios. In the orbital period versus secondary mass diagram, recurrent novae are located in different regions from classical novae and the positions of recurrent novae are consistent with the single degenerate scenario.

Keywords: novae - light curve analysis - WD mass - UV - X-rays - type Ia supernova.

1 Introduction

A nova outburst is a thermonuclear runaway event on a white dwarf (WD). After unstable hydrogen shell-burning sets in, the envelope greatly expands and the WD becomes very bright and reaches its optical maximum. After the maximum expansion of the photosphere, the WD's radius shrinks with time. Free-free emission of the expanding ejecta dominates the spectrum in the optical and infrared regions. A large part of the hydrogen-rich envelope is blown away in the wind and the photosphere gradually moves inside.

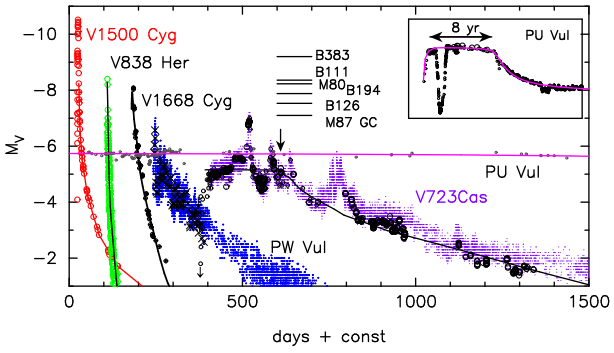

Figure 1: Light curves of various speed classes of novae. From left to right, V1500 Cyg, V838 Her, V1668 Cyg, PW Vul, V723 Cas, and PU Vul (horizontal line and inset), which are taken from Kato et al. (2013).

Figure 1 shows V and visual light curves of six well-observed Galactic classical novae with different speed classes. V1500 Cyg is an exceptionally bright (superbright), very fast nova ($t_2 = 2.9$ days and $t_3 = 3.6$ days). Here, t_2 (t_3) is the time in days in which a nova decays by two (three) magnitudes from its maximum. V838 Her is a very fast nova, one of the fastest novae except for the superbright novae. It exhibits a normal super-Eddington luminosity in the early phase. V1668 Cyg is a fast nova with $t_2 = 12$ days and $t_3 = 25$ days. PW Vul is a slow nova that exhibits oscillatory behavior in the early phase. V723 Cas is a very slow nova that features multiple peaks in the early stage. PU Vul is a symbiotic nova with a flat optical peak lasting eight years. Its light curve for the first 20 years is plotted in the inset of Figure 1.

Many classical novae exhibit super-Eddington luminosity, i.e., the peak luminosity exceeds the Eddington luminosity at the photosphere.

$$L_{\rm Edd} \equiv \frac{4\pi c G M_{\rm WD}}{\kappa}, \qquad (1)$$

where κ is the OPAL opacity. If we assume $M_{\rm WD} = 1.0\ M_\odot$ and $\kappa = 0.4$, the Eddington luminosity is $L_{\rm Edd} = 1.258 \times 10^{38}$ erg sec^{-1}.

Because of space limitations, in this paper we concentrate on the light curve analysis of the decay phase of novae and their relation to type Ia supernova (SN Ia) progenitors. For other important issues readers may re-

fer to a brief summary of super-Eddington luminosity and a theoretical explanation of maximum magnitude versus rate of decline of novae (the MMRD relation) by Kato (2012), the common path in the color-color diagram by Hachisu and Kato (2014), and information on instability of the shell flash by Kato & Hachisu (2012).

2 Nova Light Curves

2.1 The universal decline law

Decay phases of novae can be followed based on the theory of optically thick winds. In this method, we construct a sequence of steady-state solutions with assumed chemical composition of the hydrogen-rich envelope. We solve the equations of motion, mass continuity, radiative diffusion, and conservation of energy, from the bottom of the hydrogen-rich envelope through the photosphere assuming a steady-state (Kato & Hachisu 1994).

Optical and infrared light curves are calculated by assuming free-free emission originating from the optically thin ejecta outside the photosphere. The flux of free-free emission is estimated by

$$F_\nu \propto \int N_e N_i dV \propto \int_{R_{\rm ph}}^{\infty} \frac{\dot{M}_{\rm wind}^2}{v_{\rm wind}^2 r^4} r^2 dr \propto \frac{\dot{M}_{\rm wind}^2}{v_{\rm ph}^2 R_{\rm ph}}, \quad (2)$$

during the optically thick wind phase, where F_ν is the flux at frequency ν, N_e and N_i are the number densities of electrons and ions, respectively, $R_{\rm ph}$ is the photospheric radius, $\dot{M}_{\rm wind}$ is the wind mass-loss rate, $v_{\rm ph}$ is the photospheric velocity, and $N_e \propto \rho_{\rm wind}$ and $N_i \propto \rho_{\rm wind}$. These $\dot{M}_{\rm wind}$, $R_{\rm ph}$, and $v_{\rm ph}$ values are calculated from our optically thick wind solutions. Figure 2 shows light curves calculated for various WD masses. As the wind mass-loss rate quickly decreases with time, the flux at a given wavelength also decreases with time. Note that the shape of the light curve is independent of the frequency (or wavelength), whereas the absolute magnitude, i.e., proportionality constant of Equation (2), depends on it. This wavelength-free light curve shape is one of the characteristic properties of free-free emission (see Hachisu & Kato 2006). For a more massive WD, its light curve decays more quickly mainly because of its smaller envelope mass, so the evolution time scale is shorter.

These light curves follow a common shape, known as *the universal decline law*. If we plot these light curves on logarithmic time since the outburst, and shift them in the vertical and horizontal directions (i.e., normalize them in the time direction by a factor of $f_{\rm s}$ and also shift the magnitude in the vertical direction by $-2.5 \log f_{\rm s}$), all the light curves essentially converge into a single curve (Hachisu & Kato 2010) independently of the WD mass and chemical composition, as demonstrated in Figure 3. This figure also shows the UV 1455 Å narrowband light curve. This narrow band is defined observationally to avoid prominent emission and absorption lines in the nova UV spectra and to represent the continuum flux (Cassatella et al. 2002). We see that our model light curves of the UV 1455 Å band also converge into a single curve by using the same time-scaling factor of f_s. In our model light curves, X-ray turnoff times do not converge, because the supersoft X-ray phase (duration of steady nuclear burning) depends on the hydrogen burning rate, which does not follow the times-scaling law.

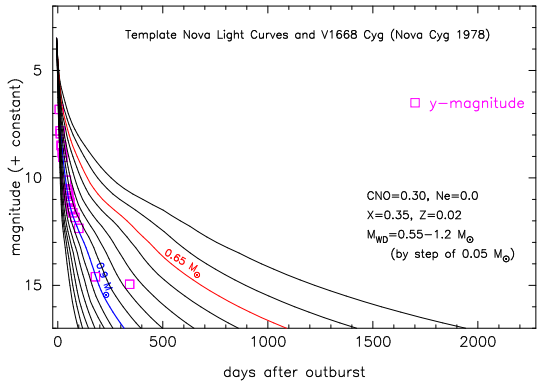

Figure 2: Free-free emission model light curves for various WD masses from 0.55 $M_\odot$ to 1.2 $M_\odot$ in steps of 0.05 $M_\odot$ (taken from Hachisu & Kato 2010). Open squares denote observational y magnitudes of V1668 Cyg that show good agreement with the 0.95 $M_\odot$ model.

This figure also shows the fundamental properties of nova evolution. After the optical maximum, the photospheric temperature rises with time, and the main emitting wavelength region shifts from optical to UV and then to supersoft X-ray. The optically thick winds continue until the photospheric temperature reaches $\log T$ (K) > 5.2 (which corresponds to the opacity peak from iron ionization). The WD photosphere emits supersoft X-rays until hydrogen nuclear burning stops. After the hydrogen burning is extinguished, the nova enters a cooling phase and finally the WD becomes dark.

Figure 4 shows the same light curves as in Figure 3 but on a real time scale. In a light curve analysis, we can select the best-fit theoretical model by comparing observed data with our model, but only the optical light curve is not enough. This is because the main body of the optical light curve follows the same decline rate of $t^{-1.75}$ and we can fit several light curves of different WD masses with the optical data as seen in Figure 4. If we have information other than optical, such as the UV 1455 Å light curve or X-ray turn-on and turnoff times,

we can accurately select one model light curve. This is why multiwavelength observations are important for determining the nova parameters.

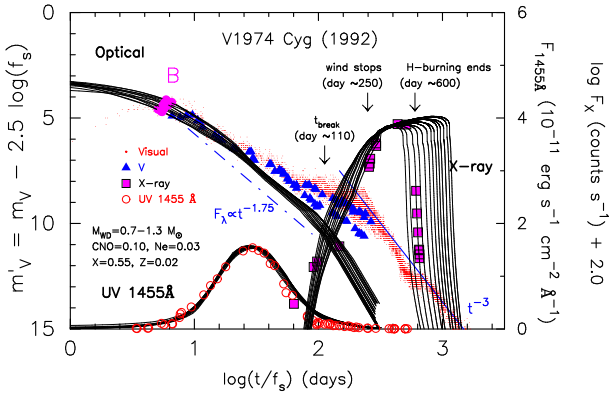

Figure 3: Free-free emission model light curves for various WD masses from 0.7 $M_\odot$ to 1.3 $M_\odot$ by steps of 0.05 $M_\odot$ (taken from Hachisu & Kato 2010). The time scales are squeezed or stretched by a factor of f_s along time to fit each other and the magnitude is shifted by $-2.5 \log f_s$. The two straight lines indicate the decline rates of free-free flux, i.e., $F_\nu \propto t^{-1.75}$ (dash-dotted line) and $F_\nu \propto t^{-3}$ (solid line). Observational data of V1974 Cyg are superposed.

2.2 Chemical composition of ejecta

Classical novae exhibit heavy element enrichment in their ejecta by a few to several tens of percent by mass (see Table 1 in Hachisu & Kato 2006 for a summary). This enhancement is considered to originate the WD by diffusion of accreted hydrogen into a core during a quiescent phase (e.g., Prialnik 1986). As the surface of a WD core is eroded during nova outbursts and blown off in the nova wind, the WD mass decreases after each nova outburst.

However, in recurrent novae, the composition of ejecta is very different from those of classical novae and is almost solar. Theoretical calculations showed that a certain amount of processed helium is added to the WD after every outburst (Prialnik & Kovetz 1995). The WD could then experience repeated weak helium shell flashes. The resultant wind is weak, and a large part of the envelope mass remains on the WD (Kato & Hachisu 2004). Therefore, the WD increases its mass in recurrent novae such as U Sco and RS Oph.

Note that helium burning produces a substantial amount of Ne and Mg (Shara & Prialnik 1994). Therefore, even if the WD is made of carbon and oxygen, the hydrogen-rich envelope could be contaminated with neon. Mason (2011) claimed that the high Ne/O line ratios observed in U Sco indicate that U Sco harbors an ONeMg WD. Mikolajewska criticized Mason's results because Mason neglected the effects of collisions on the line formation. With these effects included, the U Sco abundance is consistent with the solar abundance ratio. Mason (2013) accepted Mikolajewska's criticism and revised her results on the U Sco WD, which previously had been totally erroneous because of her misinterpretation and miscalculation. Here, we note that (1) high Ne/O line ratios could be an indication of a mass-increasing WD and (2) strong Ne lines are detected even in the slow nova V723 Cas (Iijima 2006), which harbors a low-mass WD (0.5–0.6 $M_\odot$).

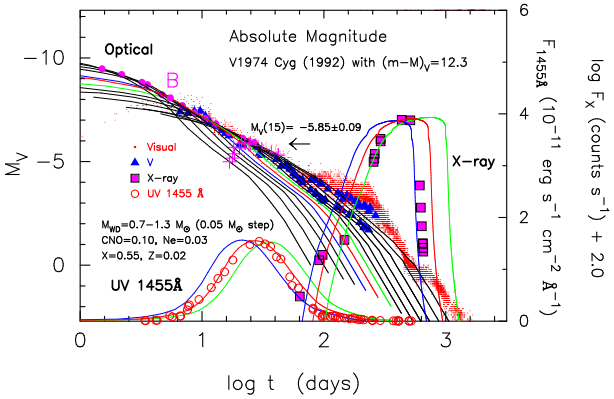

Figure 4: Same as Figure 3 but on a real time scale and using absolute V magnitude (taken from Hachisu & Kato 2010). Model UV and supersoft X-ray light curves are plotted only for three WD masses (1.1 $M_\odot$, 1.05 $M_\odot$, and 1.0 $M_\odot$) to improve readability.

2.3 WD masses estimated by light curve fittings

Figures 3 and 4 also show light curves of the classical nova V1974 Cyg. The optical light curve decays as $t^{-1.75}$ from the optical peak at $t = 2.67$ days (point B). There are two different sets of V-magnitudes obtained by using different V filters that have different degrees of emission line contamination. As the nova enters the nebular phase, strong emission lines such as [O III] contribute to the V band flux and the V magnitude becomes much brighter than the continuum flux. (The theoretical free-free flux mimics the continuum flux.) After the optically-thick winds stops, the magnitude decays as t^{-3}, which represents free-expansion of the ejecta.

Because the optical, UV, and supersoft X-ray light curves have different dependencies on the WD mass, we can choose a best-fit model that reproduces these three light curves simultaneously as shown in Figure 4. In this way, we have estimated the WD mass in many classical novae, recurrent novae, and a symbiotic nova. Such

examples are shown in Figure 1 by the solid lines that represent theoretical light curve models. These WD masses are $M_{\rm WD} = 1.20\ M_\odot$ for V1500 Cyg, 1.35 $M_\odot$ for V838 Her, 0.95 $M_\odot$ for V1668 Cyg, and 0.6 $M_\odot$ for V723 Cas.

Note that some classical novae have optical light curves that are similar to those of recurrent novae. For example, V838 Her and U Sco have very similar optical and UV 1455 Å light curves. Also the classical nova V2491 Cyg exhibits a similar optical decline to that of RS Oph. V838 Her and V2491 Cyg are classical novae and their WD masses are decreasing because of heavy element enhancement in their ejecta, whereas U Sco and RS Oph have mass-increasing WDs. This indicates that classical and recurrent novae share different histories of binary evolution even if they exhibit very similar light curves.

2.4 Very slow novae with a flat optical peak

PU Vul is a symbiotic nova that exhibits a long-lasting flat optical peak followed by a slow decline, as shown in Figure 1. The evolution of this nova can be followed by using a quasi-evolution model of an outburst on a $\sim 0.6\ M_\odot$ WD (Kato et al. 2011). In less massive WDs ($\leq 0.6\ M_\odot$, which depends slightly on the chemical composition) the optically thick winds are not accelerated and thus the nova evolution is extremely slow. In contrast, in the majority of classical novae (that occur on a WD of $M_{\rm WD} > 0.7\ M_\odot$) the strong optically thick winds are accelerated and carry most of the envelope mass in a short time. As a result, their evolutions are fast and exhibit a sharp optical maximum.

The very slow novae V723 Cas, HR Del, and V5558 Sgr exhibit a flat pre-maximum phase with no indication of a strong wind-mass loss, followed by a smooth decline with massive winds after some oscillatory phase of the optical light curves. This sequence can be understood as a transition from initial quasi-static evolution to optically thick wind evolution. The oscillatory behaviors in the light curves may correspond to a relaxation process associated with the transition from static to wind solutions (Kato and Hachisu 2011).

3 Type Ia Supernova Scenarios

Type Ia supernovae are characterized in principle by spectra without hydrogen lines but with strong Si II at maximum light. It is commonly agreed that the exploding star is a mass-accreting carbon-oxygen (C+O) WD. However, whether the WD accretes H- and He-rich matter from its binary companion (the so-called single degenerate (SD) scenario) or whether two C+O WDs merge (the so-called double degenerate (DD) scenario) has not yet been clarified.

In the DD scenario, proposed by Webbink (1984)

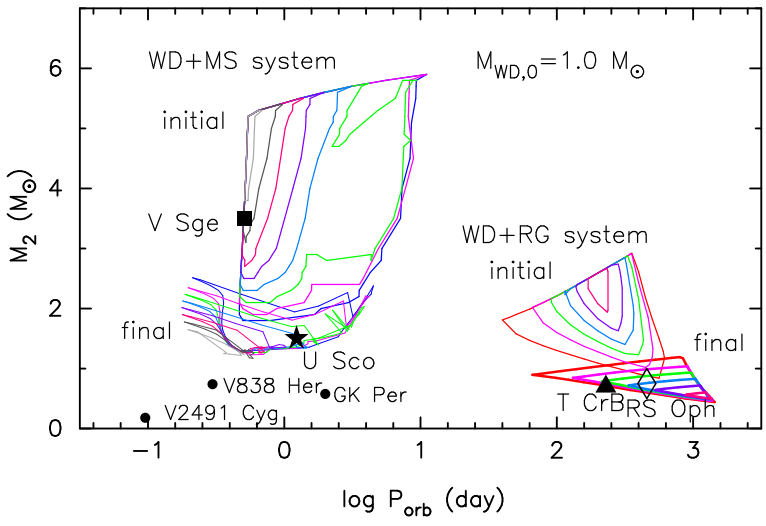

Figure 5: Initial and final binary parameter ranges for the SD scenario (taken from Hachisu et al. 2012). M_2 is the companion mass and $P_{\rm orb}$ is the orbital period. An initial binary system inside the region encircled by a solid line (labeled initial) evolves to explode as a type Ia supernova when it reaches within the region labeled final. The recurrent novae U Sco and T CrB are located inside the final region, whereas the classical novae V2491 Cyg, V838 Her, and GK Per lie outside. Most classical novae and cataclysmic variables are located much below the left-side final region.

and Iben & Tutukov (1984), intermediate-mass (3–8 $M_\odot$) binaries undergo the first and second common envelope phases and finally become a double WD system. If the orbital period is very short (i.e., if they merge within a Hubble time), and the total mass exceeds the Chandrasekhar mass, it could explode as a SN Ia. After introduction of this traditional DD scenario, many modified binary evolution scenarios have been proposed, but the evolutionary path is essentially governed by the efficiency parameter of the common envelope evolution (e.g. Webbink 2008), which is not well constrained yet.

The original idea of the SD scenario was proposed by Whelan & Iben (1973), but this idea was soon abandoned by one of its originators (Iben) in 1984 because of its too small contribution to SNe Ia. These studies are based on the old opacity, which was revised at the beginning of the 1990s. The new opacities have a large peak at $\log T$ (K) ~ 5.2, which brought drastic change in stellar structures. The presence of strong optically thick winds has changed nova theory, and we now can well reproduce observational light curves. Hachisu et al. (1996) adopted these optically-thick winds as a new elementary process in binary evolution, which was dubbed the accretion wind evolution. The WD accretes matter from the accretion disk and, at the same time, blows optically thick winds. These winds carry mass and angular momentum, so mass transfer in the binary can be stabilized, and, in most cases, the so-called second common envelope evolution does not occur. WDs can grow in mass to the Chandrasekhar mass and explode as a SN Ia. Therefore, the essential difference between the DD and SD scenarios resides in the assumption of the second common envelope evolution or accretion wind evolution. The physical process of the latter is well studied in nova outbursts, whereas the former process is not established yet (see e.g., Webbink 2008, Kato and Hachisu 2012 for more details).

3.1 WD+RG channel and WD+MS/sG channel

In the SD scenario, there are two known channels to SNe Ia, i.e., the WD+MS (including sub-giant (sG) companion) channel and the WD+RG channel.

The WD+RG channel was proposed by Hachisu et al. (1996), who called it the symbiotic channel. In this symbiotic channel we start from a very wide binary consisting of a pair of MS stars. The primary evolves to an asymptotic giant branch (AGB) star. The binaries undergo a common envelope-like evolution during the superwind phase of the primary AGB star. The orbital period of the binary shrinks to 30 – 800 days, with the binary now consisting of a CO WD and a MS star. Then the secondary MS star evolves to a RG with a helium core and fills its Roche lobe. As the mass-transfer rate exceeds the critical rate, the binary undergoes the accretion wind evolution phase. The mass-transfer rate gradually decreases and the optically thick winds stop. Then all the accreted matter is burned on the primary CO WD. The binary enters a persistent supersoft X-ray source (SSS) phase. The mass-transfer rate further decreases to below the minimum rate of steady hydrogen burning ($\dot{M}_{\rm st}$) and the binary enters a recurrent nova phase. Depending on the binary parameters, the WD mass reaches $M_{\rm WD} = 1.38\ M_\odot$ during one of the three phases (wind, SSS, and recurrent nova) and explodes as a type Ia supernova.

The MS/sG channel was proposed by Li & van den Heuvel (1997) and further investigated by Hachisu et al. (1999b) and others. In this channel, a pair of MS stars evolves to a binary consisting of a helium star plus a MS star after the first common envelope evolution. The primary helium star further evolves to a helium RG with a CO core and fills its Roche lobe followed by a stable mass-transfer from the primary helium RG to the secondary MS star. The secondary MS star increases its mass and is contaminated by the primary's nuclear burning products. The primary becomes a CO WD after all the helium envelope is transferred to the secondary MS star. Then, the secondary evolves to fill its Roche lobe and mass transfer begins from the secondary MS (or subgiant) star to the primary CO WD. Then, the system enters an accretion wind evolution phase. After that, the binary becomes a persistent SSS and evolves finally to a recurrent nova. During these three periods, the primary WD increases its mass to the Chandrasekhar mass. Depending on the binary parameters, the WD will explode as a SN Ia during one of the three phases (wind, SSS, and recurrent nova).

Some binaries are identified by the last phase of each channel. In the symbiotic channel, the SMC symbiotic X-ray source SMC3 corresponds to the SSS phase and symbiotic recurrent novae such as RS Oph and T CrB correspond to the last phase. In the MS/sG channel, V Sge and RX J0513.9−6951 correspond to the accretion wind evolution phase. Steady-burning supersoft sources such as Cal 87 and Cal 83 correspond to the SSS phase. U Sco and V394 CrA are recurrent novae in the MS/sG channel.

3.2 Evolutionary status of novae and recurrent novae

Figure 5 shows the orbital period versus secondary mass diagram for SN Ia progenitor binaries for both the WD+MS/sG channel and the WD+RG channel. The upper region labeled "initial" for each channel indicates that binaries will evolve downward with the secondary mass decreasing and the WD mass increasing and even-

tually explode as a SN Ia in the "final" region.

The present positions of U Sco and T CrB in this diagram are very consistent with the final stage. From light curve analysis, the WD mass is determined as massive as 1.37 $M_\odot$ for U Sco and 1.35 $M_\odot$ for RS Oph and T CrB. These values are also consistent with this final stage toward a type Ia SN.

In contrast, classical novae V838 Her and V2491 Cyg are located much below the final region, indicating that neither is on the way toward a SN Ia explosion in the WD+MS/sG channel nor in the WD+RG channel, even though they harbor a massive WD near the Chandrasekhar mass.

In this way, the present status of these recurrent novae and classical novae can be understood from the difference in binary evolution that is consistent with the SD scenario. However, in the original DD scenario, there are no known paths to recurrent novae, especially for the RS Oph type systems. Thus, studies of CVs are important in understanding the nature of progenitors of SNe Ia.

References

[1] Cassatella, A., Altamore, A., González-Riestra, R.: 2002, A&A 384, 1023

[2] della Valle, M.: 1991, A&A 252, 9

[3] Hachisu, I., Kato, M.: 2001, ApJ 558, 323 doi:10.1086/321601

[4] Hachisu, I., Kato, M.: 2006, ApJS 167, 59 doi:10.1086/508063

[5] Hachisu, I., Kato, M.: 2010, ApJ 709, 680 doi:10.1088/0004-637X/709/2/680

[6] Hachisu, I., Kato, M.: 2014, ApJ 785, 97 doi:10.1088/0004-637X/785/2/97

[7] Hachisu, I., Kato, M., Nomoto, K.: 1996, ApJ 470, L97

[8] Hachisu, I., Kato, M., Nomoto, K.: 1999a, ApJ 522, 487

[9] Hachisu, I., Kato, M., Nomoto, K.: 2008, ApJL 683, 127 doi:10.1086/591646

[10] Hachisu, I., Kato, M., Nomoto, K.: 2012, ApJL 756, L4 doi:10.1088/2041-8205/756/1/L4

[11] Hachisu, I., Kato, M., Nomoto, K., Umeda, H.: 1999b, ApJ 519, 314 doi:10.1086/307370

[12] Iben, I., Jr., Tutukov, A. V.: 1996, ApJS 105, 145

[13] Iijima, T.: 2006, A&A 451, 563

[14] Kato, M., Hachisu, I.: 1994, ApJ 437, 802

[15] Kato, M., Hachisu, I.: 2004, ApJ 613, L129 doi:10.1086/425249

[16] Kato, M., Hachisu, I.: 2009, ApJ 699, 1293 doi:10.1088/0004-637X/699/2/1293

[17] Kato, M., Hachisu, I.: 2011, ApJ 743, 157

[18] Kato, M, Hachisu, I.: 2012, BASI 40, 393.

[19] Kato, M., Hachisu, I., Cassatella, A., González-Riestra R.: 2011, ApJ 727, 72

[20] Kato, M, Hachisu, I., Henze, M.: 2013, ApJ, 779, 19

[21] Mason, E.: 2011, A&A 352, L11 (2013, A&A 556, C2: corrigendum)

[22] Prialnik, D.: 1986, ApJ 310, 222

[23] Prialnik, D., Kovetz, A.: 1995, ApJ 445, 789

[24] Shara, M., M., Prialnik, D.: 1994, AJ 107, 1542

[25] Webbink, R. F.: 1984, ApJ 277, 355

[26] Whelan, J., Iben, I., Jr.: 1973, ApJ 186, 1007

[27] Webbink, R. F.: 2008, ASSL 352, 233

DISCUSSION

JAN-UWE NESS: For a SN Ia, the WD has to be a CO WD, thus, the progenitor main-sequence was low mass star. Are there really enough CO WDs with high-enough initial mass? Furthermore, the companion will initially be of rather low mass in order not to evolve faster than the primary star. Can such a companion feed a lot of mass onto the CO WD until the SN Ia explosion? Thus a SD progenitor will have a very low mass companion just before SN Ia explosion.

MARIKO KATO: A CO WD originates from less massive stars (M at ZAMS $< 8\ M_\odot$). The companion mass is smaller than this value. We have calculated the binary evolution including mass exchange, mass-loss from the binary, wind mass-loss from the WD, and so on. As you see in Figure 5, the mass permitted for the secondary is rather limited. Especially in the WD+RG channel, the initial companion mass is small, i.e., 1 – 3 $M_\odot$ when the secondary had just filled its Roche lobe, and 0.5 – 1.0 $M_\odot$ just before the SN Ia explosion. For the primary WD, the initial 0.9 – 1.07 $M_\odot$ WD becomes a type Ia SN. We calculated the expected number of SNe Ia and showed that the two channels have enough SNe Ia. Their delay time distribution is also consistent with observation (Hachisu et al. 2008).

GIORA SHAVIV: We do a calculation of one flash and find that $10^{-7} M_\odot$ is accreted. Here we infer that this system will be a SN Ia. But we saw only how a $10^{-7} M_\odot$ are accreted and infer that the same is true with 0.1 $M_\odot$. This is an extrapolation over 6 orders of magnitude!! Hence can easily be wrong.

MARIKO KATO: In our estimate based on the light curve analysis, the accumulation efficiency in typical recurrent novae (U Sco and RS Oph) is about 50%. The accreted matter in one nova outburst is $1.2 \times 10^{-6} M_\odot$ for U Sco, and $1 - 2 \times 10^{-6} M_\odot$ for RS Oph. As the WD is estimated to be 1.35 $M_\odot$ for RS Oph and 1.37 $M_\odot$ for U Sco, we can expect a continuous mass increase of the WDs, not just from an extrapolation from 1.3 $M_\odot$.